Frontiers in Scientific Research and Technology

Online ISSN: 2682-2970
Print ISSN: 2682-2962
http://fsrt.journals.ekb.eg

FSRT J 10 (2025) 10 – 17 10.21608/fsrt.2024.313073.1136

The role of thermal treatments in the transition from insulating to semiconducting PANI Films: For respiration monitoring applications

Ghada El-Barbary[a], Ibrahim Morad[a], Said M. El-Sheikh[b], Y. A. Sharaby[a,*]

[a] Department of Physics, Faculty of Science, Suez University, P.O. Box:43221, Suez 43221, Egypt.

[b] Nanostructured Materials and Nanotechnology Department, Advanced Materials Institute, Central Metallurgical Research and Development Institute (CMRDI), P.O. Box: 87, Helwan, Cairo, 11421, Egypt

ARTICLE INFO

Article history:
Received 17 August 2024
Received in revised form 8 September 2024
Accepted 11 September 2024
Available online 17 September 2024

Keywords
PANI Film,
Humidity,
Conductivity,
Proton conductivity,
Energy harvesting applications

ABSTRACT

EDA (Ethylenediamine)-doped PANI films were easily prepared by the spin coating method. The films are treated at different temperatures and times, 100 ℃/4h, 150ºC/1min, 150 ℃/30min, and 150 ℃ / 1h. Several methods including FT-IR, TEM, and XRD described the characterizations of PANI films. The samples' conductivity change during human respiration was investigated. A respiration frequency of 0.3, 0.29, 0.35, and 0.354 Hz was obtained via 100 ℃ / 4h, 150 ℃ / 1 min, 150 ℃ / 30 min and 150 ℃ / 1h, respectively for adult respiration at rest, which agreed well with the previously reported values. The 100 ℃ / 4h sample distinguished every exhaling cycle and showed a clear baseline during the continuous respiration monitoring. However, in the case of a high annealing temperature and time, the samples distinguished every cycle but without a defined baseline. This demonstrates the ability of the 100 ℃ / 4h sample to determine the calm state respiration frequency of humans with a defined baseline.

1. Introduction

Nowadays, chemical sensors—which employ polymers like polyaniline (PANI)—play a significant part in environmental monitoring (air, water, etc.) for achieving a higher life standard. The earliest known synthesized organic conductive polymer is almost certainly polyaniline. The chains of PANI have two main structural units: quinoid and benzene-like. In the base form, the PANI ideal formula includes 3 benzoid units [–C_6H_4–NH–] and a quinoid unit [–N=C_6H_4=N–] [1]. PANI has a special feature that makes it distinct from other conductive polymers: reversible and direct doping–dedoping process via acid–base treatment. This enables us to tune its electrical and optical properties [2] in accordance with the PANI's molecular structure [3]. The benzoid and quinoid units could converted into each other by oxidation-reduction methods. Recently, PANI has achieved increasing attention, mainly due to the intriguing physical features that have been discovered (electrical, optical, and electro-optical) [4], and has many potential applications such as supercapacitors [5, 6], sensors [7], electronic devices [8], batteries [9] and corrosion protection in organic coatings [10]. In addition, compared to other conductive polymers, PANI is inexpensive, environmentally stable, easy to processability, and relatively simple doping on the other hand [11].This makes the PANI used in chemical vapor and toxic gas sensors [11].

* Corresponding author at Suez University

E-mail addresses: yasser_sharaby@hotmail.com (Y. A. Sharaby)

The relative humidity (RH) sensor has been used in monitoring humidity and can be utilized as a respiratory monitor tool as the exhalation has a high concentration of moister. Several monitor techniques of respiration process could be considered as healthcare monitoring devices. It can be used in noninvasive routine respiratory activity checks to help detect some serious health issues such as apnea [12], asthma [13], and chronic obstructive pulmonary diseases [14]. Based on having π-electron backbone, conducting polymers have low-energy optical transitions, high electron affinity, low ionization potential, and electrical conductivity, among other remarkable electronic characteristics [15]. Based on the distinctive structure of the conducting polymers (CPs) characterized by successive single and double bonds (π-conjugated structure). Which in turn, facilitates vapor molecules interaction with the CPs chains changing their electrical characteristics. The unique electrical characteristics attain the CPs as an appealing choice of gas or vapor sensor, which can be produced in large quantities, for applications towards gas sensing. Guodong *etal.* [16] Prepared based polyaniline wearable mask for respiration monitoring. Respiration frequency detection was determined for breathing rate monitoring applications. The sample resistance was increased by 1 kΩ in several seconds during short breath. However, the resistance was raised by 5 kΩ in time interval 15 S under deep respiration. In addition, the PANI based sensor exhibited both fast and recovery time. These findings showed that the PANI based sensor can be utilized for breath frequency determination and considered a promising candidate for health monitoring devices.

In this paper, we prepare EDA-doped annealed PANI films by facile spin coating technique. We studied the annealing temperature effect on the present film structure. Furthermore, real-time human respiration monitoring is investigated.

2. Experimental

2.1 Materials

Polyaniline powder (AG003TUD) with 99.5 % Purity was purchased from Indagoo. Ethylenediamine (EDA 107-15-3) with 99.5 % Purity and dimethylformamide (DMF) with 99.5 % Purity were purchased from ADvent.

2.2 Experimental procedure

Fig. 1 showed the schematic diagram of the EDA-doped PANI films preparation. EDA (Ethylenediamine)-doped polyaniline (PANI) films were synthesized by the spin coating facile technique. The precursor solution was made by stirring the PANI powder in DMF (Dimethylformamide) for a few minutes. Then, EDA was wisely added drop by drop to the mentioned solution while stirring till having a homogenous solution. The final solution was mid stirred (at 350 rpm) for several hours. Before the deposition on a glass substrate, the glass substrates were rinsed with distilled water and ethanol via an ultrasonic bath for 10 minutes. After the film's deposition, the films have annealed at 100 ℃ for 4 hours (100 ℃ / 4h), 150℃ for 1 minute (150 ℃ /1min), 150 ℃ for 30 minutes (150 ℃/30 min) and 150 ℃ for 1h (150 ℃ /1h). The structure of the annealed PANI samples was investigated using X-ray diffraction (Empyrean diffractometer). The morphology was investigated by transmission electron microscope (JEOL JEM 2100). Fourier transform infrared spectroscopy (FTIR) spectrum was studied using Bruker VRRTEX 80 (Germany in the range 4000 cm^{-1} – 400 cm^{-1}). The films' thickness was measured via Ellipsometer PHE – 102. The thickness was ranging between 700 and 750 nm. The change of conductivity due to nose breath (exhaling and inhaling) of the four samples is examined. A source meter model Keithley 2400 monitored the variation of the electrical current, the response signals were recorded by a Keithley 2400 source meter at 1 cm apart from the sample.

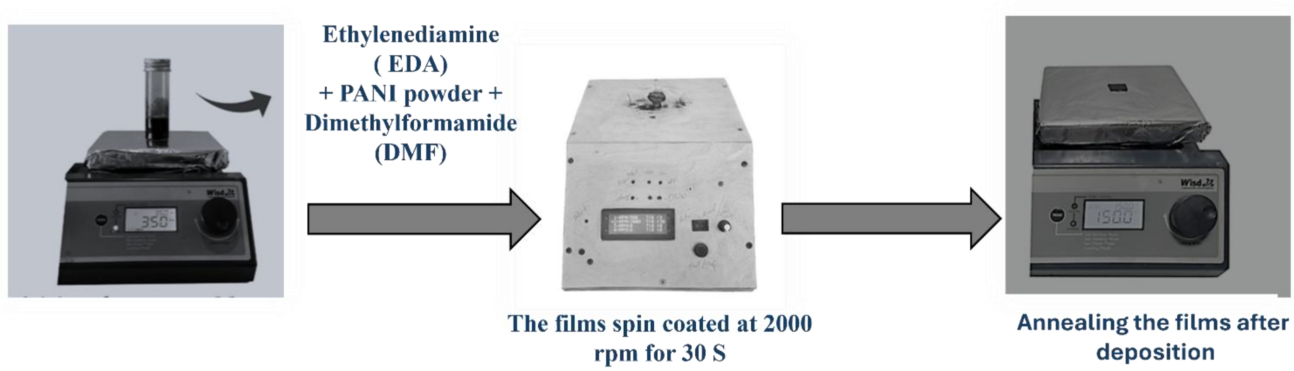

Fig. 1: Schematic illustration of the preparation of EDA-doped PANI films.

3. Results and discussion

3.1 Structural characterizations of the annealed PANI films

Fig. 2 demonstrates a typical XRD diffractogram for the four-polyaniline films with a range of angles between 5^o, and 90^o. It is declared that both the position and intensities of the samples' diffraction peaks depend on the annealing temperatures and times. The samples' X-ray pattern showed different peaks, which are anticipated to the presence of different crystalline regions and broad bands for verifying their amorphous nature. The 100^oC/4h PANI film exhibits a diffraction peak at 2θ = 25.88 agreeing the reflection from the plane (110) which may be ascribed to the parallel periodicity aligns with the polymer chains [17]. The detected peak at 2θ = 25.88 may also correspond to the reflection from the (200) plane [18], or (110 face) [19]. This representative peak at 2θ = 25.88, demonstrates the semi-crystalline nature of the 100^oC/4h PANI film. The crystallinity is beneficial for enhancing charge carriers transportation from PANI Film surface to its bulk [20]. Increasing the annealing temperature to 150 ℃ for 1 min displayed new diffraction peaks, the first one at 2θ = 20.13 relating to the reflection from the planes (020) [21] which is ascribed to parallel periodicity aligns with the polymer chains [22]. The same peak (100 face) may also distinguish the separation between the benzene ring planes of in adjacent chains (or the close-contact inter-chain distance) [23]. In addition, the other two peaks centered at 2θ = 52.43 and 59.89 also characterize polyaniline [24, 25]. Furthermore, increasing the annealing time to 30 min at the same temperature 150℃ modifies the XRD pattern. It displays a new different peak at 2θ = 7.36 and a broad peak around 2θ = 22.4. The peak at 2θ = 7.36 is a feature which characterize highly crystalline PANI structure when its polymer chains are sufficiently long and packed in high order [22, 24]. This annealing time also produces a broad hump, indicating that the condition prevents the crystallization, reduces any long-range order in that direction, and indicates a decrease in inter-chain packing. The observed broad hump exhibits a maximum of around 2θ = 22.4 which represents the separation between the benzene ring planes of in adjacent chains (or the close-contact inter-chain distance) [17]. The annealed PANI sample at 150 ℃ for 1h exhibited a similar diffraction pattern to the sample in (Fig. 1c), for temperature 150 ℃ and time 30min. It reveals a slight reduce in intensity of diffraction peak at 2θ =7.46 and a reduction in peak width. Thus, (150 ℃ /1h) sample has a lower crystallite population in that direction with a higher orientation degree of the PANI chains. As the polymer chains growth have a high degree of ordering and regularity, the polymer crystallinity exhibits more enhancements.

The annealed PANI samples extent of order length (L) for chains could be estimated using Scherrer's equation (Eq. (1)) [24]

$$L = \frac{K\lambda}{\beta \cos\theta} \quad (1)$$

Where K is equal to 0.9, β is the full width at half maximum expressed in radians, and λ (= 1.5406 Å) is the wavelength of X-rays used.

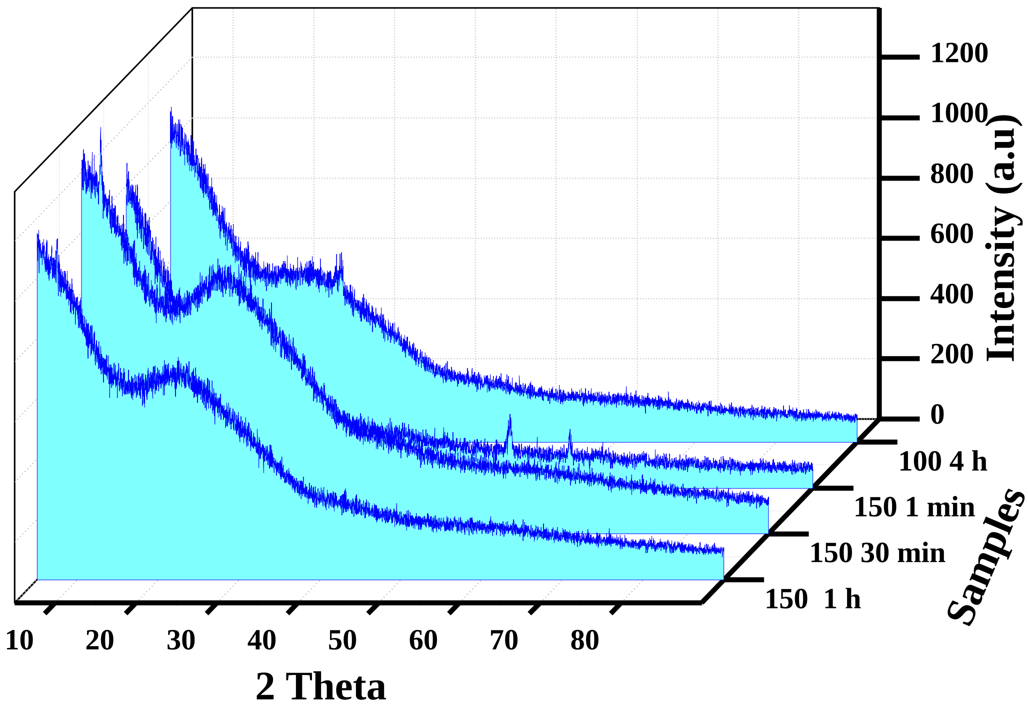

Fig. 2: X-ray diffraction spectra of the annealed PANI films

Table 1: 2θ, Crystal domain length L (nm), d- Spacing (Å) and Inter-chain separation S (Å) of the annealed PANI films.

Sample name	2θ	Crystal domain length L (nm) ± 0.01	d- Spacing (Å) ± 0.02	Inter-chain separation (Å) ± 0.02
100 °C / 4 h	25.88	6.81	3.44	4.3
150 °C / 1 min	20.13	7.94	4.41	5.51
	52.43	9.66	1.74	2.18
	59.89	7.25	1.54	1.93
150 °C / 30 min	7.36	20.16	11.99	14.99
	22.39	1.27	3.97	4.96
	27.98	0.78	3.19	3.98
150 °C / 1 h	7.46	23.39	11.84	14.8
	22.53	1.11	3.94	4.93
	28.29	0.86	3.15	3.94

For deeper investigation of the structural characteristics of the annealed PANI samples, the interplanar spacing (d) and inter-chain separation length (S) of all samples could also be calculated [24]. The value of interplanar spacing (d) was defined according to the Bragg relation Eq. 2, while the Klug and Alexander equation was used for calculation of the inter-chain separation length Eq. 3,

$$\mathbf{d} = \frac{\lambda}{2 \sin \theta} \qquad (2)$$

$$\mathbf{R} = \frac{5\lambda}{8 \sin \theta} \qquad (3)$$

Table 1 summarizes 2θ, Crystal domain length L (nm), d-Spacing (Å), and Inter-chain separation S (Å) of the annealed EDA doped PANI films at room temperature.

3.2 FTIR spectroscopy of the annealed PANI films

The Fourier transform infrared (FTIR) absorption spectrum of the synthesized PANI films has been employed to describe the structure after sample annealing at different temperatures and times. Figs. 3 display the FTIR spectra of the annealed PANI samples at different temperatures. The characteristic bands arising at wavenumber (1387-1395) cm^{-1} are assigned to the C = C stretching vibrations of quinoid while (1502-1534) cm^{-1} is assigned to the C = C vibrations of benzenoid rings absorption [26]. The detected bands around (1650-1660) cm^{-1} are associated with the C = N stretching of the quinoid ring [27]. The characteristic of aromatic amine stretching (B…C…N) is detected at (1257-1301) cm^{-1} [28]. A weak band was observed at (3047.48- 3050.94) cm^{-1} which characterize –NH2 and N–H stretching [29]. The nonbonded (N–H) stretching is detected at 3674 cm^{-1} only in Fig. 2b for 150 ℃ /1 min PANI film spectrum [27]. The detected signals appeared at (747-762) cm^{-1} was assigned to the out-of-plane bending vibration of N–H bond [29]. A weak broad bands were observed at (2880-2940) cm^{-1} indicating the C–H stretching vibrations of the PANI backbone [30]. The band at wavenumber 1090 cm^{-1} indicated the vibration for C-H in-plane bending of the aromatic ring. This band distinguish the 1, and 4 bonded positions of the benzene rings in the polymer chain backbone [31]. The detected bands at the region 700 cm^{-1} to 900 cm^{-1} are assigned to the C-H out of the plane bending vibrations deformation [31]. The band at 841 cm^{-1} is attributed to Out-of-plane C–H bending 1, 4-disubstituted benzene ring [32].

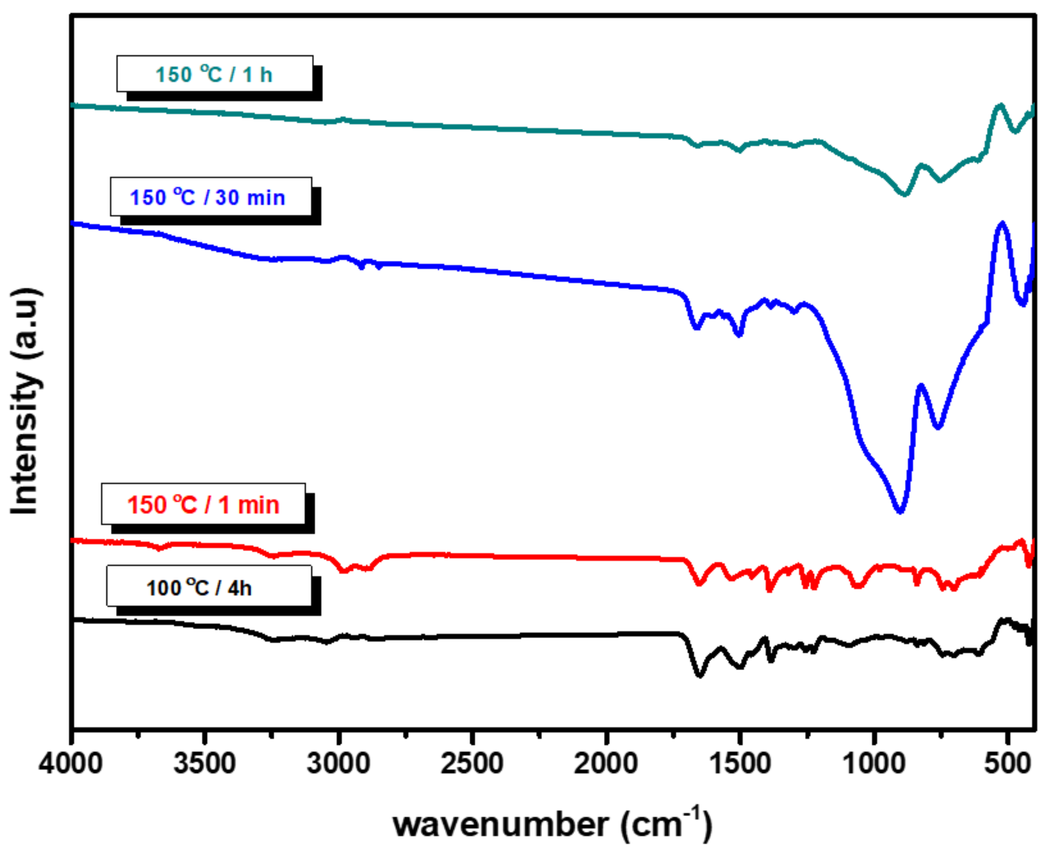

Fig. 3: FTIR spectrum of the annealed PANI films.

Peaks between (400-475) cm^{-1} are assigned to C–N–C bonding mode of the aromatic ring [29]. The FTIR spectrum of the heat-treated PANI films shows a decrease in the intensity of the peaks assigned to C = N quinoid and C= C benzenoid rings vibration absorption besides a remarkable increase in Out of plane C–H bending 1, 4-disubstituted benzene ring and N–H out-of-plane bending vibration. The intensity of the OH stretching vibration band at 3241 cm^{-1} remarkably decreased as the annealing temperature and time were increased [33].

3.2 TEM Study

TEM image of 100 ℃ / 4h annealed PANI film at 100 nm magnification is shown in Fig. 4. It displayed PANI uniformly distributed nanocrystals with crystal size ranging between (14-25) nm. Furthermore, TEM images of 100 ℃ / 4h and 150 ℃ / 1h PANI films are shown in Figs. 5a and b, respectively, for morphology investigation. TEM images of the two samples have sheet-like appearances. 100 ℃ / 4h film revealed the formation of soft-edged stacked sheets, whereas 150 ℃ / 1h film revealed agglomeration of sheets with undefined boundaries. The sheet like morphology may be one of the reasons responsible for enhancing the samples' conductivity under respiration process. As the highly surface area characterize the sheet morphology may increase the adsorption of vapor molecules during respiration process.

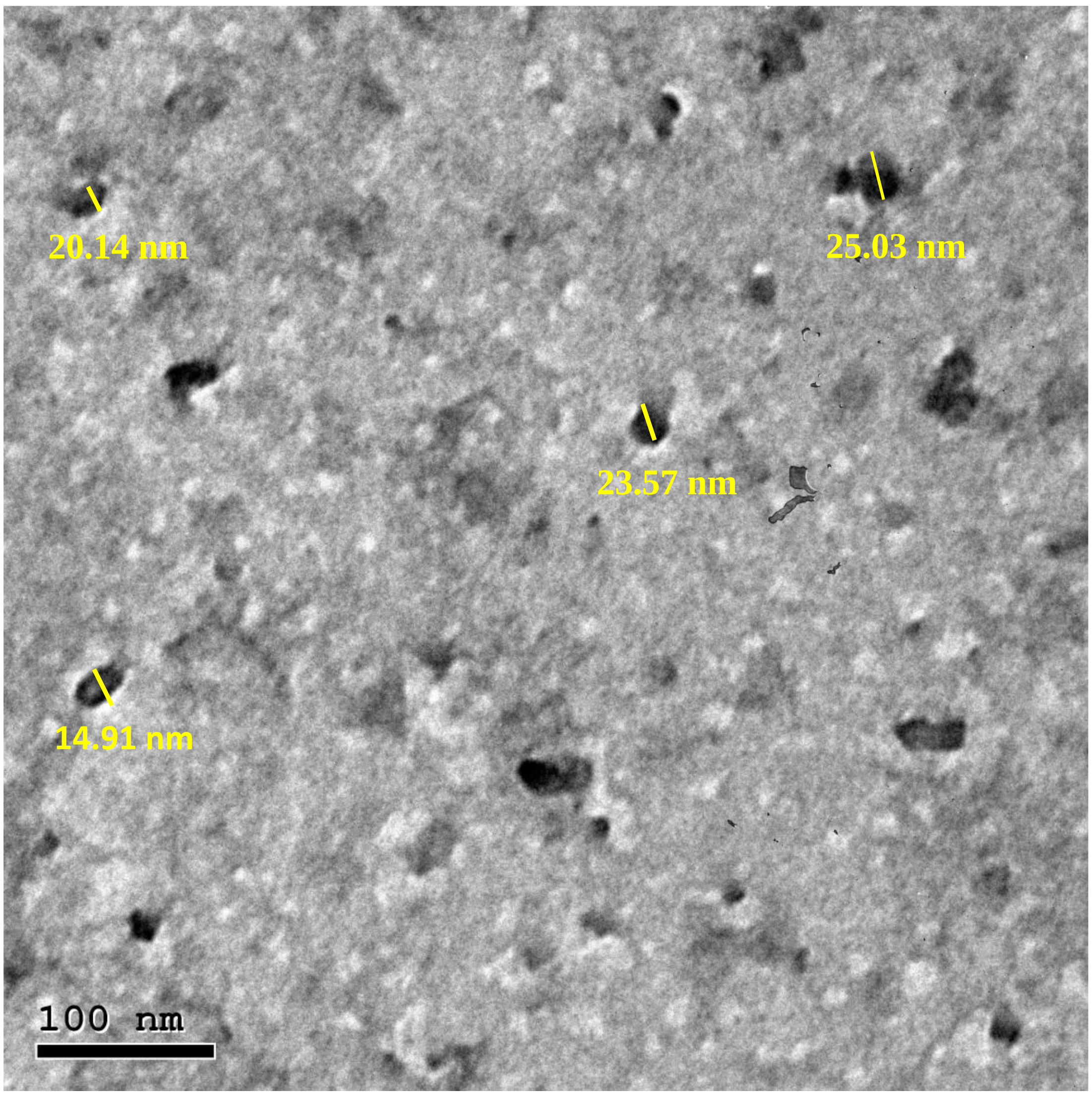

Fig. 4: TEM image of 100 ℃ / 4h annealed PANI film at 100 nm magnification.

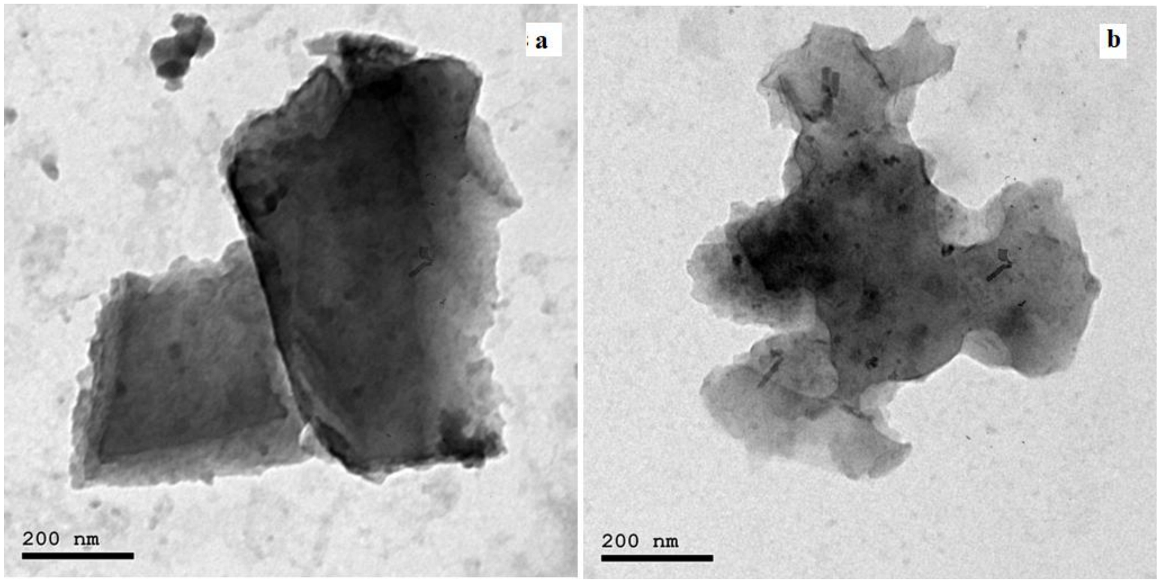

Fig. 5: TEM images of a) 100 ℃ / 4h annealed PANI film and b) 150 ℃ / 1h annealed PANI film.

3.3 Electrical conductivity transition under nose respiration

Figs. 6 (a – d) illustrates the change in conductivity of the four PANI films during respiration in the mode at rest at room temperature. The DC conductivity change of the annealed PANI films during respiration is calculated according Eq. 4 [34],

$$\boldsymbol{\sigma} = \frac{\mathbf{d}}{(\mathbf{AV})}\,\mathbf{I} \qquad \mathrm{Scm^{-1}} \qquad (4)$$

where d is the film thickness in (cm), A is the film area (cm^2), V is the potential difference across the film, and I is the current flowing through the film.

The experiment was conducted by monitoring one of the authors' nose respirations. The nasal exhalation and inhalation alter the relative humidity (RH%) of the films' ambience. This RH% change modifies the films' current data which is recorded simultaneously via source meter Keithley device. The change in conductivity of the samples due to the exposure to respiration normally at the calm normal state condition was investigated by placing the film at 1 cm from the nose. The films conductivity changed as a response to human respiration, the films were powered by the Keithley DC power source. Each respiration cycle established a response peak. A respiration frequency of 0.3, 0.29, 0.35, and 0.354 Hz was obtained from the response curves of Figs. (6 a-d) which corresponding to 100 ℃ / 4h, 150 ℃ /1 min, 150 ℃ /30 min and 150 ℃ /1h, respectively for adult respiration at a calm state, which agreed well with the reported values [30]. However, in the case of samples treated in high annealing temperature and time Figs. 6 (b-d) , the respiration of the samples distinguished every cycle without a defined baseline. The sample 100 ℃ / 4h Fig. 6 a showed a clear baseline during the continuous respiration monitoring. This demonstrates the ability of the (100 ℃ / 4h) sample to determine the calm state respiration frequency of humans with a defined baseline which is suitable for noncontact switches providing the advantage of diminishing bacterial transmission [35]. The adult respiration normal rate ranges between 12–15 breaths per minute which is equivalent to 0.20 – 0.25 Hz, respectively. This respiration rate may be raised to 60 breaths per minute (1 Hz) for hyperventilation under effect of exercise or illness [36]. The respiratory sensors can be utilized for early stage of respiration diseases prediction. Consequently, the respiration monitoring sensors should be intensively investigated to manipulate a more accurate performance. The highly PANI content films (10 % wt) and sheet like morphology increase the adsorption of vapor molecules caused by respiration. In addition, it caused a transition in samples' conductivity from insulating state to semiconducting state as illustrated in Fig. 6. The rise in conductivity through exhalation breathing may originate from intrinsic charge transport, proton hopping via water molecules (Grotthuss mechanism), and/or ionic transport in the polymer film. The modification of functional groups to the PANI backbone may support a specific interactions between the ionized group and the vapor molecules [36]. Polyaniline (PANI) has been studied for humidity responses. Matveeva et al. [37] proposed that a hydrogen bond is established between the water molecules and the polymer might enhance the intrinsic charge transport of PANI. Macdiarmid et al. [38] ascribed the conductivity enhancement due to the hopping of protons over the water molecules aligned along the polymer backbone; with subsequent dissociation in H^+ and OH^- in the film [39]. Furthermore, instead of a proton (H^+) hopping, only the charge (as an electron-hole) is transferred to a neighboring water molecule, without a net movement of the nucleus (the proton) [36].

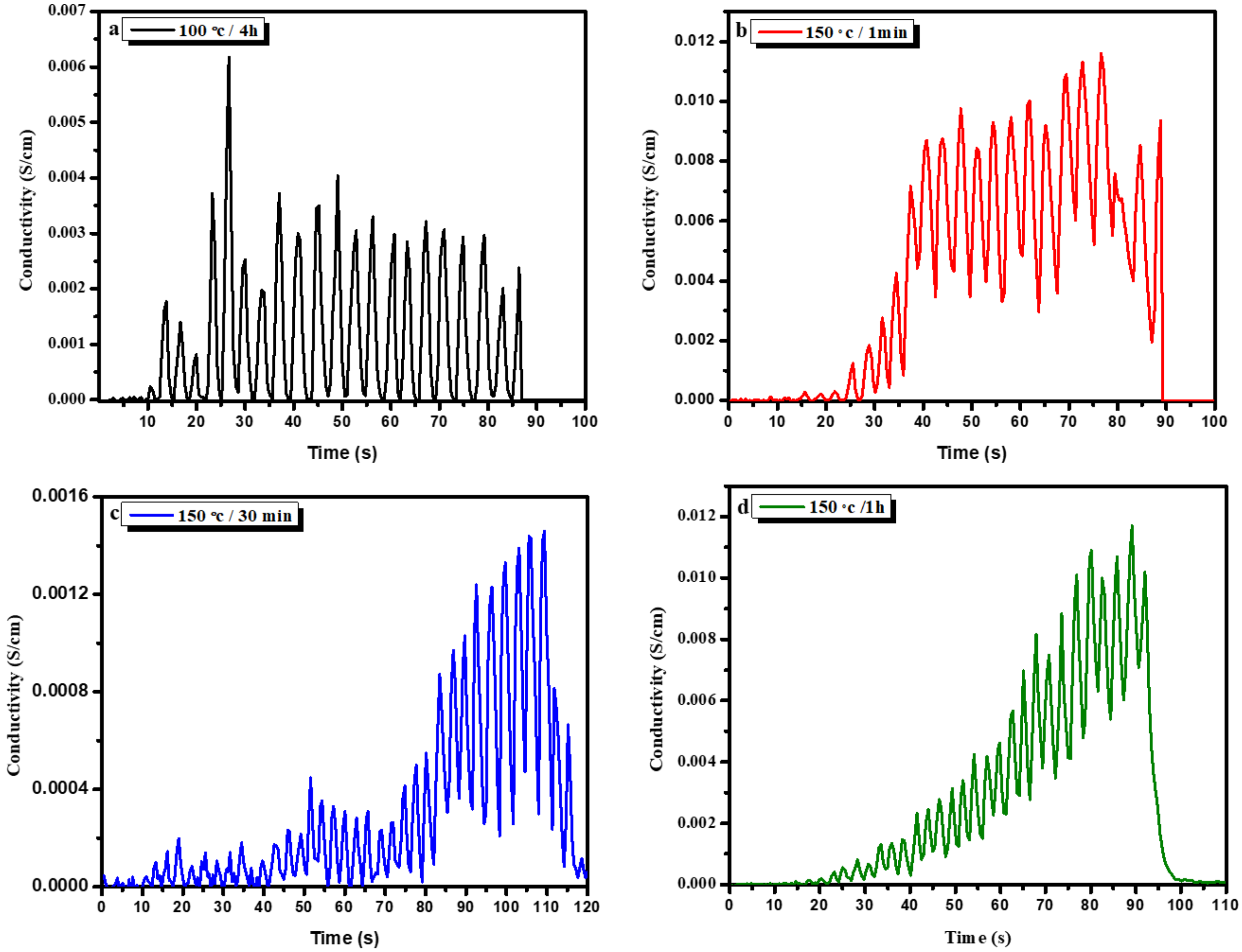

Fig. 6: Conductivity change of the a) 100 ℃ / 4h PANI film, b) 150 ℃ / 1 min PANI film, c) 150 ℃ / 30 min PANI film, and d) 150 ℃ / 1h PANI film during respiration at calm state.

Conclusion

In summary, the annealed EDA-doped PANI films were prepared by facile spin coating method. The samples were treated at a temperature of 100 ℃ for 4 hours then three samples were annealed at a temperature of 150 ℃ for different times. The treating temperature and time noticeably affect the structure of samples as revealed by XRD, FT-IR, and TEM, and the conductivity change of samples as a response to exhalation and inhalation nose respiration. All samples generate a response peak to every respiration cycle. The respiration recorded rate agrees with the previously reported values. PANI films distinguished every cycle but without a defined baseline, except sample 100 ℃ /4h showed a clear baseline during the continuous respiration monitoring. This demonstrates the ability of the 100 ℃ / 4h sample to determine the calm state respiration rate of humans with a defined baseline which is appropriate for noncontact switches and provides the benefit of reducing bacterial transmission.

Reference

1. Rangel-Vázquez, N.A., et al., Characterization of copolymer based in polyurethane and polyaniline (PU/PANI). 2009. **53**(4): p. 248-252.

2. Daikh, S., et al., Chemical polymerization, characterization and electrochemical studies of PANI/ZnO doped with hydrochloric acid and/or zinc chloride: Differences between the synthesized nanocomposites. Journal of Physics and Chemistry of Solids, 2018. **121**: p. 78-84.

3. Elizalde-Torres, J., H. Hu, and J.J.R.m.d.f. Saniger, Comparison of NO2 and NH3 gas adsorption on semiconductor polyaniline thin films. 2005. **51**(5): p. 482-487.

4. Wadatkar, N.S. and S.A. Waghuley, Characterizing the electro-optical properties of polyaniline/poly(vinyl acetate) composite films as-synthesized through chemical route. Results in Surfaces and Interfaces, 2021. **4**: p. 100016.

5. Dhawale, D.S., et al., Fuzzy nanofibrous network of polyaniline electrode for supercapacitor application. Synthetic Metals, 2010. **160**(5): p. 519-522.

6. Dubal, D.P., et al., Polyaniline–polypyrrole nanograined composite via electrostatic adsorption for high performance electrochemical supercapacitors. Journal of Alloys and Compounds, 2013. **552**: p. 240-247.

7. Deshpande, N.G., et al., Studies on tin oxide-intercalated polyaniline nanocomposite for ammonia gas sensing applications. Sensors and Actuators B: Chemical, 2009. **138**(1): p. 76-84.

8. Jia, W., et al., Polyaniline–DBSA/organophilic clay nanocomposites: synthesis and characterization. Synthetic Metals, 2002. **128**(1): p. 115-120.

9. Gurunathan, K., D.P. Amalnerkar, and D.C. Trivedi, Synthesis and characterization of conducting polymer composite (PAn/TiO2) for cathode material in rechargeable battery. Materials Letters, 2003. **57**(9): p. 1642-1648.

10. Sathiyanarayanan, S., et al., Sulphonate doped polyaniline containing coatings for corrosion protection of iron. Surface and Coatings Technology, 2010. **204**(9): p. 1426-1431.

11. Azim-Araghi, M. and M.J.T.E.P.J.A.P. Jafari, Electrical and gas sensing properties of polyaniline-chloroaluminium phthalocyanine composite thin films. 2010. **52**(1): p. 10402.

12. Tatara, T. and K. Tsuzaki, An Apnea Monitor Using a Rapid-Response Hygrometer. Journal of Clinical Monitoring, 1997. **13**(1): p. 5-9.

13. Woollard, M. and I.J.E.M.J. Greaves, 4 Shortness of breath. 2004. **21**(3): p. 341-350.

14. Oki, Y., et al., Usefulness of the 6-minute walk test as a screening test for pulmonary arterial enlargement in COPD. 2016: p. 2869-2875.

15. Lu, J., et al., Polyaniline nanoparticle–carbon nanotube hybrid network vapour sensors with switchable chemo-electrical polarity. Nanotechnology, 2010. **21**(25): p. 255501.

16. Wu, G., et al., A wearable mask sensor based on polyaniline/CNT nanocomposites for monitoring ammonia gas and human breathing. 2023. **375**: p. 132858.

17. Bandgar, D., et al., Facile and novel route for preparation of nanostructured polyaniline (PANi) thin films. 2014. **4**: p. 27-36.

18. Lenin, R., A. Singh, and C.J.J.o.M.S.M.i.E. Bera, Effect of dopants and morphology on the electrical properties of polyaniline for various applications. 2021. **32**: p. 24710-24725.

19. Souza Jr, F.G., et al., Effect of pressure on the structure and electrical conductivity of cardanol–furfural–polyaniline blends. 2011. **119**(5): p. 2666-2673.

20. Imali, D.Y., et al., Fabrication and characterization of a flexible and disposable impedance-type humidity sensor based on polyaniline (PAni). 2023. **13**(10): p. 6396-6411.

21. Niranjana, M., et al., Localized polarons in in situ synthesized polyaniline nanocomposite improve the morphology and the thermal and electrical conductivity. 2016. **6**(116): p. 115074-115084.

22. Zhu, X., et al., Structural-controlled synthesis of polyaniline nanoarchitectures using hydrothermal method. 2015. **27**(2): p. 207-216.

23. Bhandari, S. and D.J.J.o.A.P.S. Khastgir, Synergistic effect of dopant combination and switchover in formation mechanism of polyaniline nanowire. 2015. **132**(8).

24. Golba, S., et al., Impact of acidity profile on nascent polyaniline in the modified rapid mixing process—Material electrical conductivity and morphological study. 2020. **13**(22): p. 5108.

25. Hopkins, A.R., P.G. Rasmussen, and R.A. Basheer, Characterization of Solution and Solid State Properties of Undoped and Doped Polyanilines Processed from Hexafluoro-2-propanol. Macromolecules, 1996. **29**(24): p. 7838-7846.

26. Zhang, J., D. Shan, and S. Mu, Electrochemical copolymerization of aniline with m-aminophenol and novel electrical properties of the copolymer in the wide pH range. Electrochimica Acta, 2006. **51**(20): p. 4262-4270.

27. Al-Daghman, A.N.J.J.I.J.R.A.S.E.T., Optical Characteristics of Conductive Polymer Polyaniline PANI-EB. 2018. **6**: p. 1555-1560.

28. Kumar, R. and B.C. Yadav, Humidity sensing investigation on nanostructured polyaniline synthesized via chemical polymerization method. Materials Letters, 2016. **167**: p. 300-302.

29. Slimane, A.B., A.F. Al-Hossainy, and M.S.J.J.o.M.S.M.i.E. Zoromba, Synthesis and optoelectronic properties of conductive nanostructured poly (aniline-co-o-aminophenol) thin film. 2018. **29**(10): p. 8431-8445.

30. Kundu, S., et al., Relative humidity sensing properties of doped polyaniline-encased multiwall carbon nanotubes: Wearable and flexible human respiration monitoring application. 2020. **55**(9): p. 3884-3901.

31. Kulandaivalu, S., Z. Zainal, and Y.J.I.J.o.P.S. Sulaiman, Influence of monomer concentration on the morphologies and electrochemical properties of PEDOT, PANI, and PPy prepared from aqueous solution. 2016. **2016**(1): p. 8518293.

32. Abdelkader, R., H. Amine, and B.J.I.J.o.P.S. Mohammed, Thermally Stable Forms of Pure Polyaniline Catalyzed by an Acid-Exchanged Montmorillonite Clay Called Maghnite-H+ as an Effective Catalyst. 2012. **2012**(1): p. 846710.

33. Ping, Z., et al., States of water in different hydrophilic polymers—DSC and FTIR studies. 2001. **42**(20): p. 8461-8467.

34. Nagaraju, S., et al., Humidity sensing properties of surface modified polyaniline metal oxide composites. 2014. **2014**(1): p. 925020.

35. Tatara, T. and K.J.J.o.c.m. Tsuzaki, An apnea monitor using a rapid-response hygrometer. 1997. **13**: p. 5-9.

36. Folke, M., et al., Critical review of non-invasive respiratory monitoring in medical care. 2003. **41**: p. 377-383.

37. Matveeva, E.J.S.M., Residual water as a factor influencing the electrical properties of polyaniline. The role of hydrogen bonding of the polymer with solvent molecules in the formation of a conductive polymeric network. 1996. **79**(2): p. 127-139.

38. Angelopoulos, M., et al., Polyaniline: processability from aqueous solutions and effect of water vapor on conductivity. 1987. **21**(1-3): p. 21-30.

39. Cukierman, S.J.B.e.B.A.-B., Et tu, Grotthuss! and other unfinished stories. 2006. **1757**(8): p. 876-885.